BJR

https://doi.org/10.1259/bjr.20190992

Received: 26 November 2019 | Revised: 10 February 2020 | Accepted: 21 February 2020

Cite this article as:
Zopfs D, Lennartz S, Zaeske C, Merkt M, Laukamp KR, Reimer RP, et al. Phantomless assessment of volumetric bone mineral density using virtual non-contrast images from spectral detector computed tomography. *Br J Radiol* 2020; **93**: 20190992.

FULL PAPER

Phantomless assessment of volumetric bone mineral density using virtual non-contrast images from spectral detector computed tomography

[1]DAVID ZOPFS, MD, [1,2,3]SIMON LENNARTZ, MD, [1]CHARLOTTE ZAESKE, MD, [4]MARTIN MERKT, MD, [1]KAI ROMAN LAUKAMP, MD, [1]ROBERT PETER REIMER, MD, [1]DAVID MAINTZ, MD, [1]JAN BORGGREFE, MD and [1]NILS GROSSE HOKAMP, MD

[1]University of Cologne, Faculty of Medicine and University Hospital Cologne, Institute for Diagnostic and Interventional Radiology, Cologne, Germany
[2]Else Kröner Forschungskolleg Clonal Evolution in Cancer, University Hospital Cologne, Weyertal 115b, 50931, Cologne, Germany
[3]Department of Radiology, Massachusetts General Hospital, 55 Fruit St, White 270, Boston, MA 02114, USA
[4]University of Cologne, Faculty of Medicine and University Hospital Cologne, Cologne, Germany

Address correspondence to: Mr David Zopfs
E-mail: *david.zopfs@uk-koeln.de*

Objective: To evaluate phantomless assessment of volumetric bone mineral density (vBMD) based on virtual non-contrast images of arterial (VNC_a) and venous phase (VNC_v) derived from spectral detector CT in comparison to true non-contrast (TNC) images and adjusted venous phase conventional images ($CI_{V(adjusted)}$).
Methods: 104 consecutive patients who underwent triphasic spectral detector CT between January 2018 and April 2019 were retrospectively included. TNC, VNC_a, VNC_v and venous phase images (CI_V) were reconstructed. vBMD was obtained by two radiologists using an FDA/CE-cleared software. Average vBMD of the first three lumbar vertebrae was determined in each reconstruction; vBMD of CI_V was adjusted for contrast enhancement as suggested earlier.
Results: vBMD values obtained from $CI_{V(adjusted)}$ are comparable to vBMD values derived from TNC images (91.79 ± 36.52 *vs* 90.16 ± 41.71 mg/cm^3, $p = 1.00$); however, vBMD values derived from VNC_a and VNC_v (42.20 ± 22.50 and 41.98 ± 23.3 mg/cm^3 respectively) were significantly lower as compared to vBMD values from TNC and $CI_{V(adjusted)}$ (all $p \leq 0.01$).
Conclusion: Spectral detector CT-derived virtual non-contrast images systematically underestimate vBMD and therefore should not be used without appropriate adjustments. Adjusted venous phase images provide reliable results and may be utilized for an opportunistic BMD screening in CT examinations.
Advances in knowledge: Adjustments of venous phase images facilitate opportunistic assessment of vBMD, while spectral detector CT-derived VNC images systematically underestimate vBMD.

INTRODUCTION

It is estimated that osteoporosis causes over 9 million fractures worldwide and affects 28 million people just in the European Union.[1,2] Osteoporosis is linked to an increased mortality risk and a decreased health-related quality-of-life.[3,4] Although it is a common disease with increasing prevalence due to an aging population, it is frequently underdiagnosed.[5,6] Thus, up to 78% of all individuals with osteoporosis do not receive appropriate treatment in order to prevent fractures and reduce associated health risks.[7]

Dual-energy X-ray absorptiometry (DXA) is considered the gold-standard to assess areal bone mineral density (BMD).[8,9] Here, T- and Z-scores are used to depict results, whereby the T-score indicates the number of standard deviation difference from a healthy young population and the Z-score represents the deviation from an age-matched population.[8] Yet, DXA is apparently under used as only around 30% of females and 4% of males above the age of 65 undergo a DXA study.[10,11] Further, the diagnostic capability of DXA is limited as it is susceptible to degenerative changes and patient size.[12–14] Quantitative CT (QCT) is a well-established and widespread method to evaluate reduced BMD and allows a relative risk prediction for osteoporotic fractures.[13,15] QCT determines the volumetric bone mineral density (vBMD), which is expressed in units of mg/cm^3.[8] However, dedicated QCT to evaluate possible osteoporosis is more expensive and results in a

higher radiation exposure in comparison to DXA.[16] Beside the conventional QCT approach, which requires a simultaneous scan of a calibration phantom in a non-contrast examination, phantomless techniques are available.[13,17,18] These phantomless techniques mostly compute the vBMD based on an synchronous intrinsic calibration, *i.e.* reference measurements in the paraspinal muscle and subcutaneous fat.[5,13] Nevertheless, this intrinsic calibration has been validated for unenhanced CT scans, only. As intravenous contrast agent administration causes changes of CT attenuation (reflected in Hounsfield units, HUs) it affects measurements using phantomless vBMD methods, in body CT most examinations require contrast enhancement. Among all body CT examinations, venous-phase images (CI_V) comprise the most abundant examination. Therefore, different correction formulas have been suggested and validated for CI_V[13,17,18]; yet, calculating BMD values adjusted for contrast enhancement ($CI_{V(adjusted)}$) for each examination is time-consuming and prone to errors which hampers clinical implementation of vBMD assessment. Especially, elderly patients with suspected or known malignant disease and a consequently increased risk of osteoporotic fractures frequently undergo clinically indicated body CT and therefore may benefit from early detection of osteoporosis. This so-called opportunistic screening for osteoporosis is considered to be a promising tool in clinical routine.[5,19–21]

Material-specific measurements using a dual-layer based approach to dual-energy CT, so-called spectral detector CT (SDCT), have recently received increasing attention.[22–24] If an SDCT scanner is used for image acquisition it enables the reconstruction of virtual non-contrast images of arterial phase images (VNC_a) and venous phase images (VNC_v) in addition to conventional CT images. Virtual non-contrast images have been proven to be helpful in various clinical settings, such as the detection of biliary stones and in characterization of renal cysts.[25–27] As several studies showed an excellent correlation between dual-energy CT derived virtual non-contrast images and true non-contrast images (TNC),[28–31] virtual non-contrast images (VNC) seem a promising tool to determine vBMD and to screen for osteoporosis using phantomless techniques as described above. Further, VNC images may allow for a patient-specific contrast adjustment. Thus, the purpose of this study was to evaluate vBMD measurements based on SDCT-derived VNC_a and VNC_v reconstructions to the established reference standards TNC and $CI_{V(adjusted)}$).

METHODS AND MATERIALS

Patient collective

This study was approved by the institutional review board, written informed consent was waived due to its retrospective character. The radiological information and picture archiving and communication system was queried for patients eligible for study inclusion fulfilling following criteria:

(1) Age ≥ 18 years.
(2) Contrast-enhanced, triphasic abdominal SDCT with TNC, arterial phase and venous phase images
(3) Examination between January 2018 and April 2019

Exclusion criteria

Patients were excluded if vertebrae L1–L3 were not displayed in all acquisitions. Further, patients who underwent vertebral fusion surgery or exhibited fractures, metastases or osteolysis of any other etiology in vertebrae L1–L3 were excluded.

Imaging protocol

All CT scans were conducted as required for the patients' management and for routine clinical indications on a spectral detector dual-energy CT (IQon, Philips Healthcare, Best, The Netherlands). All patients were scanned in supine position and examined with a triphasic abdominal scanning protocol consisting of a non-contrast phase, an arterial phase and a portal venous phase with enabled tube current modulation (DoseRight 3D-DOM, Philips Healthcare, Best, The Netherlands). Detailed scan parameters are given in electronic Supplementary Table 1. In all patients, 100 ml of iodinated contrast media were administered intravenously with a flow rate of 3.5 $ml\,s^{-1}$. Bolus tracking technique was used to trigger image acquisition after reaching a threshold value of 150 HU in the descending aorta. For arterial and venous phase images, the scan was started with a delay of 16 and 50 s after reaching the threshold, respectively.

Post-processing and image setup

For vBMD measurements, conventional and VNC images of the arterial and venous phase were reconstructed from the same spectral data set. All images were reconstructed using a dedicated spectral reconstruction algorithm with a constant kernel (Spectral B, Philips Healthcare, Best, The Netherlands) using the vendor's image viewing and processing software (Intellispace Portal 9.0, Philips, Best, The Netherlands). The conventional images reconstructed with this algorithm have been shown to be identical with the images reconstructed with the vendor's hybrid-iterative reconstruction algorithm (iDose 4, Philips Healthcare, Best, The Netherlands).[32] A slice thickness of 2 mm and a section increment of 1 mm were chosen.

Bone mineral density measurements

All measurements were performed using a dedicated plugin for phantomless vBMD measurements (Intellispace Portal 9.0, Philips, Best, the Netherlands) according to the software manual and analogous to previous studies,[13,33] (Figure 1): Using multiplanar reformatting, the axial plane parallel to the end plate of the corresponding vertebrae was angulated. Here, three ellipsoid volumes of interests were drawn within the vertebral bodies: (i) in the trabecular compartment of the vertebral body, avoiding the cortical bone as well as any focal lytic or sclerotic lesions; (ii) in the paravertebral muscles (musculus erector spinae) and (iii) in the dorsal subcutaneous fat. The first three lumbar vertebrae (L1–L3) were analyzed in every patient and average vBMD values were calculated.

To evaluate inter-rater reliability, all measurements were conducted independently by two radiologists. Further, a single region of interest (ROI) was placed in the psoas muscle; here, average and attenuation and standard deviation were recorded. The latter was considered to be indicative of image noise.

Figure 1. Volumetric bone mineral density measurement at the second lumbar vertebrae. To calibrate Houndsfield units, density measurements of adjacent fat and muscle tissue were used.

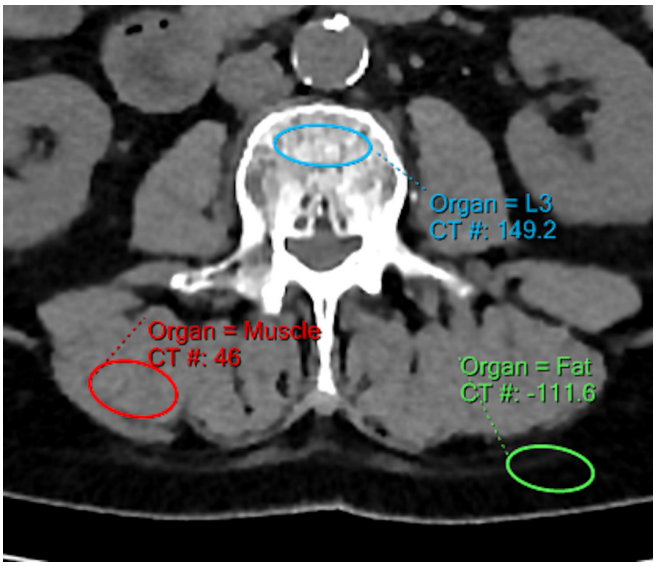

Statistics

JMP Software was used for statistical testing (v. 14, SAS Institute, Cary, USA). To adjust for contrast enhancement in venous phase images and calculate $CI_{V(adjusted)}$ following earlier suggested conversion formula was used: vBMD ($CI_{V(adjusted)}$)=0.88 × vBMD (CI_V) +4.56 mg/cc.[13] Continuous variables are provided as mean ± standard deviation. Inter-rater variability was determined using the intraclass correlation coefficient. Statistical significance was defined as $p \leq 0.05$.

RESULTS

Patient characteristics

Of the 129 patients potentially eligible for study inclusion, 25 patients were excluded due to metastasis and spondylodesis. In the final analysis 104 patients were included, of which 69 were male and 35 were female. Median age was 66 (36 – 91) years.

Attenuation and image noise

The mean attenuation between contrast enhanced CI_V and referring non-contrast reconstructions (TNC, VNC_a and VNC_v) differed significantly (all $p \leq 0.01$, Table 1). Between all non-contrast reconstructions, no significant differences in attenuation within the psoas muscle were observed ($p > 0.05$, Table 1).

Image noise was significantly lower in both VNC reconstructions and TNC as compared to CI_V (all $p \leq 0.01$, Table 1).

Measurement of vBMD

CI_V tended to overestimate average vBMD as compared to TNC (99.12 ± 41.50 *vs* 90.16 ± 41.71 mg/cm^3, $p = 0.33$, Table 2, Figure 2) while differences between $CI_{V(adjusted)}$ and TNC were negligible (91.79 ± 36.52 *vs* 90.16 ± 41.71 mg/cm^3, $p = 1.00$, Table 2, Figure 2).

Opposed to TNC and $CI_{V(adjusted)}$, average vBMD computed from VNC_a and VNC_v was significantly lower (both $p \leq 0.01$). However, vBMD computed from VNC_a and VNC_v correlated highly with those computed from TNC (adjusted r^2: 0.83 and 0.82 respectively). No significant differences were found amongst vBMD values from VNC_a and VNC_v (42.20 ± 22.50 *vs* 41.98 ± 23.31, $p = 1.00$, Table 2, Figure 2).

Inter-rater agreement was excellent (intraclass correlation coefficient >0.8).

DISCUSSION

This study evaluated virtual non-contrast reconstructions of venous and arterial phase images derived from SDCT for assessment of volumetric bone mineral density. vBMD was measured using a phantomless approach with synchronous internal calibration. vBMD values of VNC_a and VNC_v were compared to TNC and $CI_{V(adjusted)}$, which were corrected for contrast enhancement by using previously suggested equations. We found that virtual non-contrast reconstructions systematically underestimate vBMD as compared to TNC and $CI_{V(adjusted)}$.

In accordance with previous studies, our results showed a reliable removal of iodine in muscle tissue in SDCT-derived VNC reconstructions, as no significant differences in attenuation were found between TNC and VNC_a as well as between TNC and VNC_v within in the psoas muscle.[28,29,31] The lower image noise in both, arterial and venous VNC as comparised to $CI_{V(adjusted)}$ is in accordance with a study by Sauter et al, that found a markedly lower image noise in SDCT-derived VNC reconstructions in comparison to conventional images.[28] This is in line with earlier studies reporting, that spectral reconstructions from SDCT demonstrate different noise characteristics as compared to conventional image reconstructions.[28,32] These differences are likely to influence the phantomless, ROI-based approach of vBMD assessment and therefore they may partly explain the

Table 1. Attenuation and image noise

	TNC	*CI_V*	*VNCa*	*VNCv*
Mean attenuation (psoas muscle)	42.9 ± 7.2	52.2 ± 7.7*	43.5 ± 6.5	44.6 ± 6.4
Image noise (psoas muscle)	17.12 ± 0.62	21.76 ± 0.62*	16.33 ± 0.62	16.44 ± 0.62

CI, conventional image; TNC, true non-contrast; VNC, virtual non-contrast.
Mean attenuation in the psoas muscle in Hounsfield units with corresponding standard deviation (upper line) and associated image noise in the psoas muscle with corresponding standard deviation in TNC phase, venous phase (CI_V) and VNC of arterial and venous phase images (VNC_a and VNC_v respectively). Asterisk indicates statistical significance compared to TNC images.

Table 2. Volumetric bone mineral density values from different reconstructions

	TNC	*CI_V*	*$CI_{V(adjusted)}$*	*VNC_a*	*VNC_v*
Average vBMD (in mg/cm³)	90.16 ± 41.71	99.12 ± 41.50	91.79 ± 36.52	42.20 ± 22.50	41.98 ± 23.31

CI, conventional image; TNC, true non-contrast; VNC, virtual non-contrast.
Average volumetric bone mineral density in mg/cm3 measured in venous phase images (CI_V), CI_V with correction for contrast enhancement ($CI_{V(adjusted)}$), in TNC images and in VNC images of the arterial (VNC_a) and venous phase (VNC_v).

observed differences in vBMD values between VNC reconstructions and TNC as well as $CI_{V(adjusted)}$.

Another likely reason for the underestimation of vBMD from VNC reconstructions may be limits of spectral separation between iodine and calcium. Imperfect separation between iodine and calcific bone due to similar attenuation characteristics is a well-known problem inherent to the concept of dual energy CT.[28,34] Both, iodine and calcium are highly attenuating materials. Albeit, it is expected that iodine shows greater attenuation as compared to calcium, particularly in lower energies. This difference may be obscured due to system imperfections in dual energy CT resulting in removal of calcium-containing voxels in VNC images.[35,36] Particularly, it is expected that such erroneous removal occurs in lower concentrations as present in trabecular bone where the measurement is performed in phantomless vBMD assessment. The finding that differences in vBMD from VNC and TNC are independent of contrast phase indicates that the actual removal of calcific-voxels may be causal for the observed underestimation. Further, we found a high correlation between vBMD values derived from both VNC_a and VNC_v and the corresponding reference standard TNC, which indicates a systematic error due to an imperfect iodine removal in trabecular bone. It is expected, that the tendency of underestimation of vBMD measurements using VNC images applies to other available dual energy CT (DECT) approaches as well; however, it remains elusive to what extent.[32,37]

Figure 2. Average volumetric bone mineral density values derived from TNC images, venous phase images (V-CI), V-CI with correction for contrast enhancement (V-CI_adj), and from VNC images of the arterial (VNC_art) and venous phase (VNC_ven). CI,conventional image; TNC, true non-contrast; VNC, virtual non-contrast.

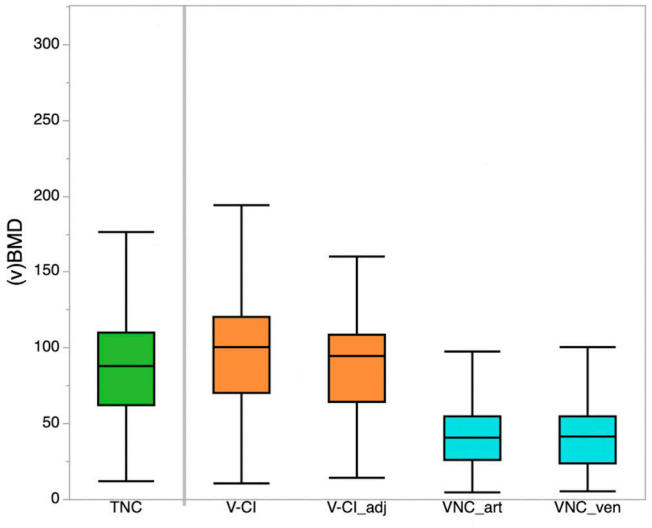

Opportunistic screening for decreased vBMD using CT is gaining increasing attention and recent studies suggest equivalence of opportunistic CT and DXA.[5,10] However, the majority of CT examinations are conducted with intravenous contrast agent, which distorts vBDM measurements in comparison to TNC. Thus, for phantomless CT with synchronous internal calibration, correction formulas have been suggested in different studies.[13,18,33] In line with these studies, we found comparable vBMD values of corrected $CI_{V(adjusted)}$ and TNC, no significant differences were found. We aimed to simplify the utilization of a phantomless opportunistic CT by means of VNC reconstructions, which might enable a patient-specific adjustment for contrast enhancement, which is varying interindividually. Further, the application of VNC images would make the usage of potential error-prone and generalized correction formulas superfluous. However, we observed relevant differences in vBMD values from VNC reconstructions and TNC / $CI_{V(adjusted)}$. It is questionable, if correction formulas for SDCT-derived VNC reconstructions are useful in clinical routine, though this could be the subject of future studies.

There are several limitations to this study that need to be addressed. First, despite the wide-spread and firmly established use of phantomless assessment of vBMD in CT examinations, we did not correlate our findings to the reference standard areal BMD measurements by DXA, as these data were unavailable for our patient cohort. Second, we solely conducted ROI-based measurement in the psoas muscle as several earlier reports on the general functionality of VNC images from SDCT are available.[28,29,31] Last, we did not perform a cross-vendor comparison. As the technological approaches to DECT differ fundamentally from each other, there are differences in spectral separative capability to be expected; however, it remains elusive if the smaller overlap in emission-based DECT approaches or the less noise in SDCT results in superiority of one over the other in the context of spectral separation.[32]

To conclude, our study revealed that VNC reconstructions derived from SDCT significantly underestimate average vBMD; inducing a risk of overdiagnosis if used without further correction. Instead, our data suggest using earlier proposed correction formulas for estimation of vBMD from contrast enhanced data.

CONFLICTS OF INTEREST

Nils Grosse Hokamp, Jan Borggrefe and David Maintz have received speakers's honoraria from Philips Healthcare. Nils Grosse Hokamp and Simon Lennartz received institutional research support from Philips Healthcare for research not related to this manuscript.

FUNDING

Parts of this study have been supported by the Else Kröner-Fresenius Stiftung (2016-Kolleg-19 to Simon Lennartz and 2018_EKMS.34 to Nils Grosse Hokamp) and by the Koeln Fortune Program / Faculty of Medicine, University of Cologne (339/2018 to Nils Grosse Hokamp).

REFERENCES

1. Hernlund E, Svedbom A, Ivergård M, Compston J, Cooper C, Stenmark J, et al. Osteoporosis in the European Union: medical management, epidemiology and economic burden. A report prepared in collaboration with the International osteoporosis Foundation (IOF) and the European Federation of pharmaceutical industry associations (EFPIA). *Arch Osteoporos* 2013; **8**: 136. doi: https://doi.org/10.1007/s11657-013-0136-1
2. Johnell O, Kanis JA. An estimate of the worldwide prevalence and disability associated with osteoporotic fractures. *Osteoporos Int* 2006; **17**: 1726–33. doi: https://doi.org/10.1007/s00198-006-0172-4
3. Hallberg I, Bachrach-Lindström M, Hammerby S, Toss G, Ek A-C. Health-related quality of life after vertebral or hip fracture: a seven-year follow-up study. *BMC Musculoskelet Disord* 2009; **10**: 135. doi: https://doi.org/10.1186/1471-2474-10-135
4. Pisani P, Renna MD, Conversano F, Casciaro E, Muratore M, Quarta E, et al. Screening and early diagnosis of osteoporosis through X-ray and ultrasound based techniques. *World J Radiol* 2013; **5**: 398–410. doi: https://doi.org/10.4329/wjr.v5.i11.398
5. Lenchik L, Weaver AA, Ward RJ, Boone JM, Boutin RD. Opportunistic screening for osteoporosis using computed tomography: state of the art and argument for paradigm shift. *Curr Rheumatol Rep* 2018; **20**: 74. doi: https://doi.org/10.1007/s11926-018-0784-7
6. Scientific Group Meeting on Prevention and Management of Osteoporosis, Weltgesundheitsorganisation, WHO Scientific Group Meeting on Prevention and Management of Osteoporosis. *Prevention and management of osteoporosis: Report of a WHO scientific group ; [WHO Scientific Group Meeting on Prevention and Management of Osteoporosis, Geneva, 7 - 10 April*. Geneva: World Health Organization; 2003.
7. Häussler B, Gothe H, Göl D, Glaeske G, Pientka L, Felsenberg D. Epidemiology, treatment and costs of osteoporosis in Germany--the BoneEVA Study. *Osteoporos Int* 2007; **18**: 77–84. doi: https://doi.org/10.1007/s00198-006-0206-y
8. Heidari B, Khashayar P, Rezai Homami M, Pajouhi A, Soltani A, Larijani B. Dual-energy X-ray absorptiometry diagnostic discordance between Z-scores and T-scores in a young Iranian population. *Med J Islam Repub Iran* 2014; **28**: 151.
9. Lane NE. Epidemiology, etiology, and diagnosis of osteoporosis. *Am J Obstet Gynecol* 2006; **194**(2 Suppl): S3–11. doi: https://doi.org/10.1016/j.ajog.2005.08.047
10. Laugerette A, Schwaiger BJ, Brown K, Frerking LC, Kopp FK, Mei K, et al. DXA-equivalent quantification of bone mineral density using dual-layer spectral CT SCOUT scans. *Eur Radiol* 2019; **29**: 4624–34. doi: https://doi.org/10.1007/s00330-019-6005-6
11. Curtis JR, Carbone L, Cheng H, Hayes B, Laster A, Matthews R, et al. Longitudinal trends in use of bone mass measurement among older Americans, 1999-2005. *J Bone Miner Res* 2008; **23**: 1061–7. doi: https://doi.org/10.1359/jbmr.080232
12. Bolotin HH. DXA in vivo BMD methodology: an erroneous and misleading research and clinical gauge of bone mineral status, bone fragility, and bone remodelling. *Bone* 2007; **41**: 138–54Available from. doi: https://doi.org/10.1016/j.bone.2007.02.022
13. Abdullayev N, Neuhaus V-F, Bratke G, Voss S, Große Hokamp N, Hellmich M, et al. Effects of contrast enhancement on In-Body calibrated Phantomless bone mineral density measurements in computed tomography. *J Clin Densitom* 2018; **21**: 360–6. doi: https://doi.org/10.1016/j.jocd.2017.10.001
14. Link TM. Osteoporosis imaging: state of the art and advanced imaging. *Radiology* 2012; **263**: 3–17. doi: https://doi.org/10.1148/radiol.12110462
15. Heuck AF, Block J, Glueer CC, Steiger P, Genant HK. Mild versus definite osteoporosis: comparison of bone densitometry techniques using different statistical models. *J Bone Miner Res* 1989; **4**: 891–900. doi: https://doi.org/10.1002/jbmr.5650040614
16. Damilakis J, Adams JE, Guglielmi G, Link TM. Radiation exposure in X-ray-based imaging techniques used in osteoporosis. *Eur Radiol* 2010; **20**: 2707–14. doi: https://doi.org/10.1007/s00330-010-1845-0
17. Kaesmacher J, Liebl H, Baum T, Kirschke JS. Bone mineral density estimations from routine multidetector computed tomography: a comparative study of contrast and calibration effects. *J Comput Assist Tomogr* 2017; **41**: 217–23. doi: https://doi.org/10.1097/RCT.0000000000000518
18. Toelly A, Bardach C, Weber M, Gong R, Lai Y, Wang P, et al. Influence of contrast media on bone mineral density (BMD) measurements from routine contrast-enhanced MDCT datasets using a Phantom-less BMD measurement tool. *Rofo* 2017; **189**: 537–43. doi: https://doi.org/10.1055/s-0043-102941
19. Pickhardt PJ, Pooler BD, Lauder T, del Rio AM, Bruce RJ, Binkley N. Opportunistic screening for osteoporosis using abdominal computed tomography scans obtained for other indications. *Ann Intern Med* 2013; **158**: 588–95. doi: https://doi.org/10.7326/0003-4819-158-8-201304160-00003
20. Roski F, Hammel J, Mei K, Baum T, Kirschke JS, Laugerette A, et al. Bone mineral density measurements derived from dual-layer spectral CT enable opportunistic screening for osteoporosis. *Eur Radiol* 2019; **29**: 6355–63. doi: https://doi.org/10.1007/s00330-019-06263-z
21. Alacreu E, Moratal D, Arana E. Opportunistic screening for osteoporosis by routine CT in southern Europe. *Osteoporos Int* 2017; **28**: 983–90. doi: https://doi.org/10.1007/s00198-016-3804-3
22. Lennartz S, Abdullayev N, Zopfs D, Borggrefe J, Neuhaus V-F, Persigehl T, et al. Intra-individual consistency of spectral detector CT-enabled iodine quantification of the vascular and renal blood pool. *Eur Radiol* 2019; **29**: 6581–90. doi: https://doi.org/10.1007/s00330-019-06266-w
23. Mei K, Schwaiger BJ, Kopp FK, Ehn S, Gersing AS, Kirschke JS, et al. Bone mineral density measurements in vertebral specimens

and phantoms using dual-layer spectral computed tomography. *Sci Rep* 2017; **7**: 17519. doi: https://doi.org/10.1038/s41598-017-17855-4

24. van Hamersvelt RW, Schilham AMR, Engelke K, den Harder AM, de Keizer B, Verhaar HJ, et al. Accuracy of bone mineral density quantification using dual-layer spectral detector CT: a phantom study. *Eur Radiol* 2017; **27**: 4351–9. doi: https://doi.org/10.1007/s00330-017-4801-4
25. Connolly MJ, McInnes MDF, El-Khodary M, McGrath TA, Schieda N. Diagnostic accuracy of virtual non-contrast enhanced dual-energy CT for diagnosis of adrenal adenoma: a systematic review and meta-analysis. *Eur Radiol* 2017; **27**: 4324–35. doi: https://doi.org/10.1007/s00330-017-4785-0
26. Bae JS, Lee DH, Joo I, Jeon SK, Han JK. Utilization of virtual non-contrast images derived from dual-energy CT in evaluation of biliary stone disease: virtual non-contrast image can replace true non-contrast image regarding biliary stone detection. *Eur J Radiol* 2019; **116**: 34–40. doi: https://doi.org/10.1016/j.ejrad.2019.04.008
27. Kessner R, Große Hokamp N, Ciancibello L, Ramaiya N, Herrmann KA. Renal cystic lesions characterization using spectral detector CT (SDCT): added value of spectral results. *Br J Radiol* 2019; **92**: 20180915. doi: https://doi.org/10.1259/bjr.20180915
28. Sauter AP, Muenzel D, Dangelmaier J, Braren R, Pfeiffer F, Rummeny EJ, et al. Dual-layer spectral computed tomography: virtual non-contrast in comparison to true non-contrast images. *Eur J Radiol* 2018; **104**: 108–14. doi: https://doi.org/10.1016/j.ejrad.2018.05.007
29. Ananthakrishnan L, Rajiah P, Ahn R, Rassouli N, Xi Y, Soesbe TC, et al. Spectral detector CT-derived virtual non-contrast images: comparison of attenuation values with unenhanced CT. *Abdom Radiol* 2017; **42**: 702–9. doi: https://doi.org/10.1007/s00261-016-1036-9
30. Toepker M, Moritz T, Krauss B, Weber M, Euller G, Mang T, et al. Virtual non-contrast in second-generation, dual-energy computed tomography: reliability of attenuation values. *Eur J Radiol* 2012; **81**: e398–405. doi: https://doi.org/10.1016/j.ejrad.2011.12.011
31. Jamali S, Michoux N, Coche E, Dragean CA. Virtual unenhanced phase with spectral dual-energy CT: is it an alternative to conventional true unenhanced phase for abdominal tissues? *Diagn Interv Imaging* 2019; **100**: 503–11. doi: https://doi.org/10.1016/j.diii.2019.04.007
32. Große Hokamp N, Gilkeson R, Jordan MK, Laukamp KR, Neuhaus V-F, Haneder S, et al. Virtual monoenergetic images from spectral detector CT as a surrogate for conventional CT images: unaltered attenuation characteristics with reduced image noise. *Eur J Radiol* 2019; **117**: 49–55. doi: https://doi.org/10.1016/j.ejrad.2019.05.019
33. Neuhaus V, Abdullayev N, Hellmich M, Krämer S, Maintz D, Krug B, et al. Association of quality and quantity of bone metastases and computed tomography volumetric bone mineral density with prevalence of vertebral fractures in breast cancer patients. *Clin Breast Cancer* 2016; **16**: 402–9. doi: https://doi.org/10.1016/j.clbc.2016.05.010
34. Borggrefe J, Neuhaus V-F, Le Blanc M, Grosse Hokamp N, Maus V, Mpotsaris A, et al. Accuracy of iodine density thresholds for the separation of vertebral bone metastases from healthy-appearing trabecular bone in spectral detector computed tomography. *Eur Radiol* 2019; **29**: 3253–61. doi: https://doi.org/10.1007/s00330-018-5843-y
35. Abdullayev N, Große Hokamp N, Lennartz S, Holz JA, Romman Z, Pahn G, et al. Improvements of diagnostic accuracy and visualization of vertebral metastasis using multi-level virtual non-calcium reconstructions from dual-layer spectral detector computed tomography. *Eur Radiol* 2019; **29**: 5941–9. doi: https://doi.org/10.1007/s00330-019-06233-5
36. Neuhaus V, Lennartz S, Abdullayev N, Große Hokamp N, Shapira N, Kafri G, et al. Bone marrow edema in traumatic vertebral compression fractures: diagnostic accuracy of dual-layer detector CT using calcium suppressed images. *Eur J Radiol* 2018; **105**: 216–20. doi: https://doi.org/10.1016/j.ejrad.2018.06.009
37. Hokamp NG, Maintz D, Shapira N, Chang DH, Noël PB. Technical background of a novel detector-based approach to dual-energy computed tomography. *Diagn Interv Radiol* 2020; **26**: 68–71. doi: https://doi.org/10.5152/dir.2019.19136